ISBN: 978-3-95450-231-8 ISSN: 2673-5490 doi: 10.18429/JACoW-IPAC2023-THPL126

TOWARDS FIBER OPTICS-GUIDED SYNCHROTRON RADIATION-BASED LONGITUDINAL BEAM DIAGNOSTICS AT THE KARA BOOSTER SYNCHROTRON

M.-D. Noll*, E. Bründermann, C. Goffing, D. El Khechen, S. Maier, J. L. Steinmann, C. Widmann and A.-S. Müller, Karlsruhe Institute of Technology, Karlsruhe, Germany

Abstract

Before injection into the Karlsruhe Research Accelerator (KARA), the 2.5 GeV electron storage ring at KIT, the beam energy is ramped up from 53 MeV to 500 MeV by a booster synchrotron. The whole booster is located in a concrete enclosure inside the storage ring and thus is not accessible during operation. For the study of longitudinal beam dynamics a cost-effective solution to leverage the synchrotron radiation emitted at the booster bending magnets is desired. To ensure durability of the setup and to not obstruct the removable concrete ceiling of the booster enclosure, it is required to place the radiation-sensitive readout electronics outside of the booster enclosure and outside of the storage ring. In this contribution a fiber-optic setup consisting of commercially available optical components, such as collimators, optical fibers and high bandwidth photodetectors is used. As a proof-of-concept we present experimental results of different components characterized at the visible light diagnostics port of the storage ring KARA. In addition, we report on first booster measurements along with planned future experiments.

INTRODUCTION

We investigate if optical telecom fibers, such as step index or gradient index (GRIN) fibers, and fiber-coupled photo detectors can be employed for longitudinal diagnostics in low energy synchrotrons, such as the KARA booster or cSTART [1].

SYNCHROTRON RADIATION SOURCE MODEL

The software Synchrotron Radiation Workshop (SRW)[2] is used to simulate the spectral density (see Fig. 1) and the transversal intensity profile of the synchrotron radiation (see Fig. 2) emitted through the window of one booster bending magnet. For the dipole magnets and electron beam parameters the horizontal emittance ($\epsilon_x = 165$ nm rad) and vertical emittance ($\epsilon_y = 11$ nm rad) are taken from measurements in [3], while the beam sizes are calculated according to [4]

$$\sigma_u = \sqrt{\epsilon_u \beta_u + \eta_u^2 \sigma_\delta^2} \tag{1}$$

with $\beta_x = 3.5$ m, $\beta_y = 5.5$ m, the dispersion $\eta_x = 1$ m, $\eta_y \approx 0$ and the momentum spread $\sigma_\delta = 3 \times 10^{-4}$, which yields $\sigma_x = 835$ µm and $\sigma_y = 630$ µm.

* marvin-dennis.noll@kit.edu

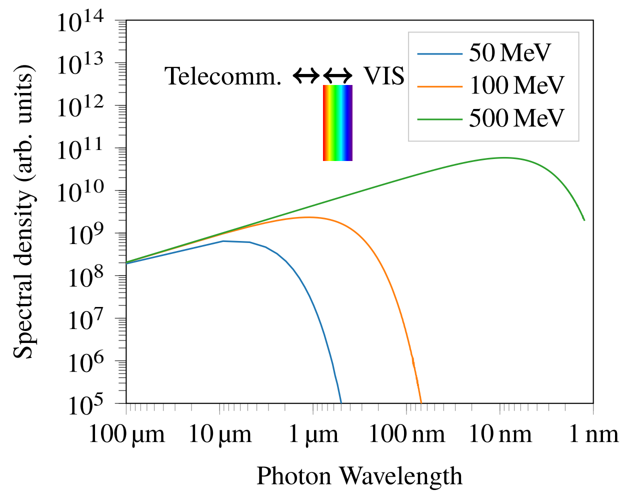

Figure 1: Spectral density of bending radiation at the booster dipole for different electron energies.

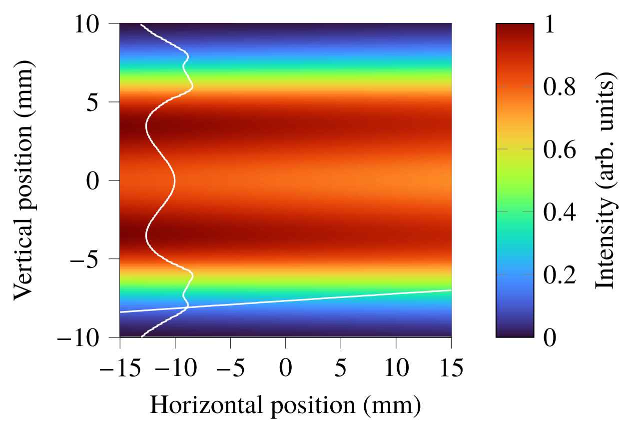

Figure 2: Transversal intensity profile of the bending magnet radiation before the synchrotron light port window (projections on the coordinate axis shown in white) at $E = 500$ MeV and for $\lambda = 700$ nm to 1600 nm.

PHOTODETECTOR SELECTION

A fiber-coupled photodetector, based on a InGaAs photodiode, is used as its spectral sensitivity in the 750 nm to 1650 nm range fits typical wavelengths of optical telecom equipment (850 nm to 1550 nm) and the synchrotron radiation spectrum of the booster. The selected DXM30BF detector features a high bandwidth (BW) of 30 GHz, which allows not only bunch-resolved measurements, but also capturing the structure of the longitudinal bunch profiles. The

ISBN: 978-3-95450-231-8 ISSN: 2673-5490 doi: 10.18429/JACoW-IPAC2023-THPL126

lower frequency limit of 0 Hz prevents a baseline shift. With the given noise equivalent power NEP = 40 pW/$\sqrt{\text{Hz}}$, the minimal detectable average power over the full bandwidth is [5]

$$P_{\text{min}} = \text{NEP}\sqrt{BW} \approx 6.9\,\mu\text{W}. \tag{2}$$

OPTICAL FIBER SELECTION

The used optical fibers have to match the 50 µm OM4 multimode-fiber FC/PC pigtail used in the DXM30BF detector. Two custom-made patch fibers are compared:

1. FG050LGA (step, 50 µm core, 0.22 NA, low-OH)
2. GIF625 (GRIN, 62.5 µm core, 0.275 NA, OM1)

Both are 35 m long and FC/APC terminated, which makes usage of FC/PC-FC/APC adapter-fibers mandatory. Both types are specified to be used in the λ = 800 nm to 1600 nm range and come with no specified dispersion ratings.

Modal dispersion is typically the dominant dispersion fraction of step index fibers. Calculating the fiber's normalized frequency V

$$V_{\text{FG050LGA}} = \frac{2\pi a}{\lambda}\sqrt{n_1^2 - n_2^2} \tag{3}$$

with a = 50 µm, λ = 1550 nm, n_1 = 1.4585, and n_2 = 1.4418 yields $V \approx 45$. The time difference between center ray and the slowest edge ray can be used to estimate a worst-case dispersion. This is a valid approach if $V \gg 10$ is fulfilled. The time difference τ for the FG050LGA fiber is calculated as

$$\Delta\tau_{\text{FG050LGA}} = \frac{L(n_1 - n_2)}{c}\left(1 - \frac{\pi}{V}\right) \approx 1.8\,\text{ns}. \tag{4}$$

The dispersion for both fibers is experimentally determined by an impulse response measurement with a short-pulse laser. Figure 3 shows the GIF625 fiber only broadens the pulse mildly, while the FG050LGA step index fiber causes the pulse to become almost six times longer. Comparison of the fiber attenuation in their respective datasheets shows a 6 dB km^{-1} difference between them, which is confirmed by the measurements shown in Fig. 3. High attenuation and the dispersion in the order of the 2 ns bunch separation time renders the FG050LGA fiber unusable, thus GIF625 is used.

OPTICAL FIBER COUPLING

To couple the synchrotron radiation from free space to the optical fiber, a concentrator setup is required. Fiber optics collimators integrate a focusing lens with a fiber connector. These are typically optimized for parallel input beams, for which

$$D_{\text{beam}} = 2\,f\,\text{NA} \Leftrightarrow f = \frac{D_{\text{beam}}}{2\,\text{NA}} \tag{5}$$

gives the (ray optics approximate) optimal focal length f of the collimator.

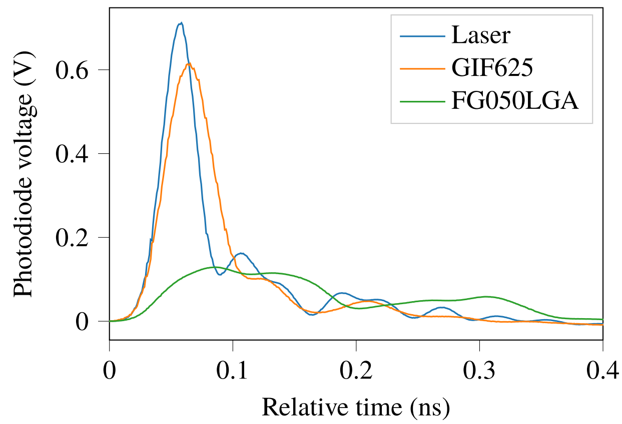

Figure 3: Optical pulses at laser output and after optical fibers; measured with DXM30BF photodiode (note: Laser only and GIF625 signals are limited by the ≈ 30 ps impulse responses of the 16 GHz digitizer used).

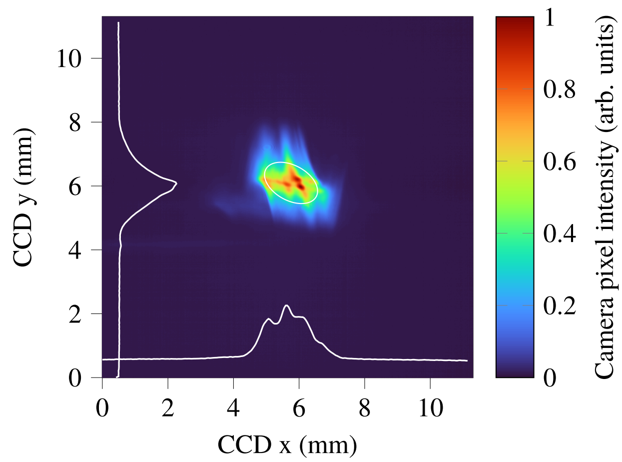

Figure 4: Intensity profile of the synchrotron radiation at the KARA beamline, taken at the collimator location.

Here, a Thorlabs F950FC-A collimator with f = 9.9 mm and an entrance aperture of D_{coll} = 11 mm is used. Its geometry does not match Eq. 5 and the fixed distance between the lens doublet and the optical fiber does not allow focusing. This requires additional optical elements to collimate the divergent beam from the synchrotron first.

EXPERIMENTAL SETUP

Before mounting the setup in the booster enclosure, tests at the more accessible 2.5 GeV KARA beamline for visible light diagnostics are performed. Due to the divergent nature of the beam, focusing mirrors and lenses are necessary to reduce the beam waist diameter. Because etendue in the optical phase space is conserved in a lens system[6], only a compromise between small beam size and low divergence angle can be achieved. With cylinder lenses, the ratio of the beam waist sizes in the horizontal and vertical planes is brought to about unity at the fiber collimator, see Fig. 4 and note the almost round Gaussian fit.

ISBN: 978-3-95450-231-8 ISSN: 2673-5490 doi: 10.18429/JACoW-IPAC2023-THPL126

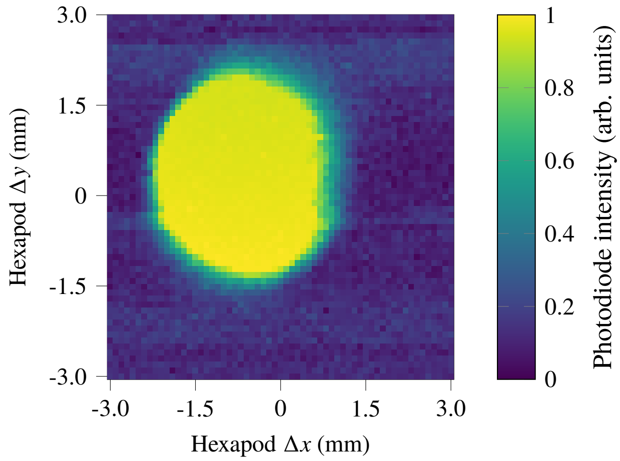

Figure 5: Normalized intensities for different fiber collimator position offsets at KARA beamline.

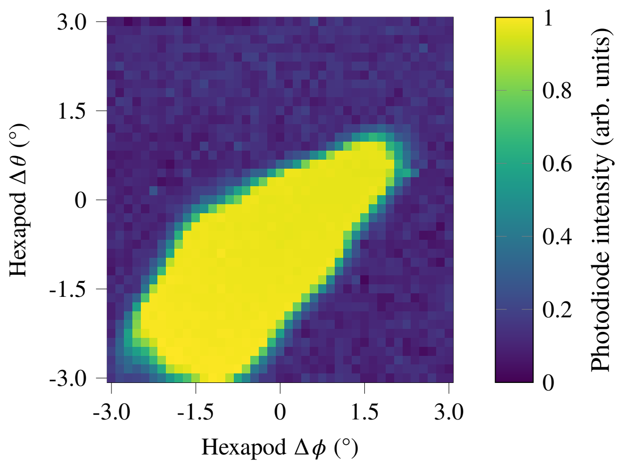

Figure 6: Normalized intensities for different fiber collimator rotations offsets at KARA beamline.

Using a 6-degree-of-freedom hexapod motion platform, the collimator is scanned in the 2D lateral (Fig. 5) and in angular (Fig. 6) space to get an optimal coupling position.

Measurements at the Booster

The measurements are repeated at the synchrotron light window at the KARA booster. Here the fiber collimator is used without additional optics. A lock-in amplifier, synchronized to $f_{\mathrm{rev,bo}} = 11.36\,\mathrm{MHz}$, is used to achieve a sufficient signal to noise ratio. On a connected oscilloscope a periodic signal repeating with the injection frequency of 1 Hz would be expected, but is not observed. Against noise and interferences, a background measurement is done with the photodiode and a non-transparent cover and a lock-in amplifier time constant of 300 ms is chosen. For both time signals, spanning 3 min each, their spectra are calculated and logarithmically subtracted from one another. This reveals no data from the synchrotron radiation. Because of that, in order to align the fiber collimator to the beam, a slow laser power meter is used instead of the photodiode and

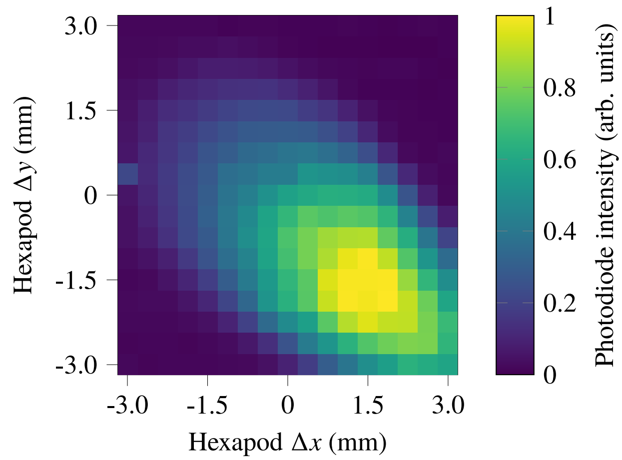

Figure 7: Normalized power meter values for different fiber collimator position offsets at KARA booster.

lock-in amplifier setup. Scanning the fiber collimator across the window results in the intensity profile in Fig. 7. After placing the collimator at the optimal position, a scan in the angular space is performed and the collimator rotated to the optimal angles. Repeating the measurement with the photodiode/lock-in-amplifier setup however, shows only noise again.

CONCLUSION AND OUTLOOK

We showed commercial gradient index optical fibers and fast telecom detectors are able to detect synchrotron radiation at high energies. But first results at the booster show that for low energy synchrotrons, off-the-shelf fiber collimators without additional optics capture too little light to achieve usable signal-to-noise ratios.

We aim for refining the collimation system by a combination of SRW for the source model and numerical optics optimizers. Other possibilities to enhance the signal to noise ratio, such as fibers with higher transmission at lower wavelengths, are also planned.

ACKNOWLEDGEMENTS

The authors acknowledge the support of the staff at the KIT IBPT mechanical workshop. S. Maier acknowledges the support by the Doctoral School "Karlsruhe School of Elementary Particle and Astroparticle Physics: Science and Technology".

REFERENCES

[1] A. I. Papash, E. Bründermann, A.-S. Mueller, R. Ruprecht, and M. Schuh, "Design of a Very Large Acceptance Compact Storage Ring", in *Proc. IPAC'18*, Vancouver, Canada, Apr.-May 2018, pp. 4239–4241. doi:10.18429/JACoW-IPAC2018-THPMF071

[2] O. Chubar and P. Elleaume, "Accurate and Efficient Computation of Synchrotron Radiation in the Near

ISBN: 978-3-95450-231-8 ISSN: 2673-5490 doi: 10.18429/JACoW-IPAC2023-THPL126

Field Region," 1998. http://cds.cern.ch/record/858849

[3] L. Præstegaard, "Investigations of the anka injector: Lattice, beam properties and performance," *Institute for Storage Ring Facilities*, Ph. D. thesis, University of Aarhus, 2001.

[4] H. Wiedemann, *Particle Accelerator Physics*, Springer International Publishing, 2015. doi:10.1007/978-3-319-18317-6

[5] V. Mackowiak, J. Peupelmann, Y. Ma, and A. Gorges, "Nep – noise equivalent power," *Thorlabs White Papers*, 2015.

[6] R. Winston, *Nonimaging optics*, lsevier Academic Press, 2005, p. 497.